A. C. Ratzel and J. E. Shepherd 1985 "Heat Transfer Resulting from Premixed Combustion," in *Heat Transfer in Fire and Combustion Systems*, (Eds. C. K. Law, Y. Jaluria, W. W. Yuen and K. Miyasaka), Publication HTD-45 of the ASME, NY, NY, 191–201.

HEAT TRANSFER RESULTING FROM PREMIXED COMBUSTION[a]

A. C. Ratzel and J. E. Shepherd
Fluid and Thermal Sciences Department 1510
Sandia National Laboratories
Albuquerque, New Mexico

Abstract

This paper considers the problems associated with modeling heat transfer resulting from combustion of hydrogen–air–steam mixtures in confined vessels. Included in this work are discussions of scaling as related to modeling radiative and convective heat transfer following completion of combustion. Results are provided from combustion tests performed in intermediate- and large-scale vessels having 5.6 m^3 and 2084 m^3 volumes, respectively. Local heat transfer data from calorimetry are shown to compare well with global estimates inferred from the gas pressure for nominal 10% hydrogen (by volume) deflagrations in these test facilities. These data are also compared with results obtained from simple scaling relations and with simulations using a nuclear reactor safety computer program, HYBER. Differences in the postcombustion gas cooling for the two different test volumes are demonstrated, pointing out the importance of scale.

Nomenclature

A	Vessel surface area
C_v	Gas specific heat at constant volume
g	Gravitational acceleration
h	Convective coefficient
k	Gas thermal conductivity
L	Convective length scale
$\mathcal{L}$	Radiation length scale
ℓ_{nc}	Intrinsic natural convection scaling length
P	Gas pressure
q	Heat flux
R	Gas constant
S	Characteristic vessel length scale
t	Time
T	Temperature
ΔT	Temperature difference
U	Gas free-stream velocity
V	Vessel volume
$\bar{x}$	Gas composition

Greek

α	Gas thermal diffusivity
α_g	Gas absorptance
β	Gas coefficient of volumetric expansion
ϵ_g	Gas emittance
ν	Gas viscosity
ρ	Gas density
σ	Stefan-Boltzmann constant
τ	Characteristic time scale

Subscripts

c	Convective
$cond$	Condensation
fc	Forced convection
g	Gas
i	Different heat transfer mechanisms
m	Maximum or AIC condition
nc	Natural convection
r	Radiative
t	Total
tc	Transient convection
w	Wall
0	Precombustion condition

[a]This work was supported by the U. S. Nuclear Regulatory Commission and performed at Sandia National Laboratories which is operated for the U. S. Department of Energy under contract number DE-AC04-76DP00789.

1 Introduction

There has been increased interest in the past five years in understanding hydrogen–air combustion processes and the attendant heat transfer mechanisms as a result of the loss-of-coolant accident at the Three Mile Island Unit 2 (TMI-2) nuclear power plant. In this accident, hydrogen was generated from reactions between the uncovered reactor core zircaloy cladding and the steam. This hydrogen was ultimately ignited in the containment building, resulting in an over-pressure of nearly 200 kPa[1]. Although this deflagration did not threaten the TMI-2 containment integrity, there has been concern by the Nuclear Regulatory Commission (NRC) that such an accident could be more serious in other reactor containments and could damage safety-related equipment. As part of reactor licensing procedures, the NRC now requires owners of certain reactor types to show that in the event of a degraded core accident involving hydrogen, mitigation systems will prevent damage to equipment that could impair a safe recovery. Deliberate ignition systems have been included in several reactor containments to burn the hydrogen at low concentrations (< 6–8% by volume), and water-spray systems in containment, if operating, are also expected to provide sufficient gas cooling to limit thermal loads which might otherwise lead to equipment failure.

The nuclear industry has been involved in experimental programs and computational studies to better quantify combustion-induced thermal environments and effects on safety-related equipment. Premixed hydrogen–air–steam combustion experiments have been performed in test vessels ranging in size from fractions of cubic meters (Mini-FITS[2] at Sandia National Laboratories (SNLA), Albuquerque, NM) to several thousand cubic meters (hydrogen dewar[3] at Nevada Test Site (NTS)). These different test facilities have provided an extensive data base for combustion in small- to large-scale vessels. These facilities, however, are still significantly smaller (at least an order of magnitude) than the large open regions of most nuclear reactors. In addition, the internal geometry of these vessels is quite different from nuclear plant containments so that the results from combustion tests in such vessels may not be appropriate for assessing equipment survivability.

Instead, computer codes such as HECTR[4] and HYBER[5] have been developed to simulate the effects of degraded-core accidents in nuclear containment buildings. Such simulations use conventional steady-state heat and mass transfer correlations and a control-volume approach to model flows between individual compartments comprising the reactor containment. Validation of these codes has been difficult, given the complexity of the degraded-core accident sequence, the difficulty in defining the time and place of ignition, and the combustion path in containment. Instead, experimental results from the simpler and smaller-scale geometries have been used to assess the ability of such codes to quantify the important heat transfer and fluid dynamic phenomena.

In this work, the problems associated with modeling heat transfer following combustion are addressed. Simple, global scaling relations for radiative and convective heat transfer are discussed, and the effects of vessel size and internal geometry on the heat transfer rates and subsequent gas cooling are shown. Representative experimental results from two 10% hydrogen deflagrations in intermediate- and large-scale facilities (5.6 and 2084 m^3 volumes, respectively) are provided to emphasize the geometry/scale effects on the postcombustion gas cooling. Comparisons of results from the simple scaling law models are given for the two experiments, as are simulations of these experiments using HYBER. Times for which radiation and convection energy transfer are important are estimated, and the need for better transient convection correlations is demonstrated.

2 Scaling

Introductory Remarks

Scaling for lean hydrogen-air deflagrations is a problematic issue that is more often avoided than not. One difficulty is in the identification of the correct nondimensional parameters and a physical basis for relating these parameters to the scale of the experiment. This difficulty arises because the characteristic fluid velocity induced by combustion is a complex and unknown function of vessel size and geometry. The velocity is also highly transient, decaying rapidly following the completion of the burn. This behavior makes it difficult to properly model the transient convective heat transfer immediately after the burn. Another difficulty is the large size of reactor containments. Even for phenomena in which the scaling parameters are well understood, *e.g.*, thermal radiation heat transfer, there are very little or no data available for length scales comparable to those in a full-sized containment building. It is possible that at large scales, a completely different physical process than that observed at small scale will dominate some of these phenomena.

The actual process by which heat is transferred from the gas to the vessel walls involves simultaneous radiation and convection. These processes are potentially strongly coupled, especially for mixtures containing high steam fractions. However, since it is difficult to treat these problems at the level of spatial detail needed to resolve this coupling, most modelers treat these processes separately and calculate the total heat transfer rate as the sum of each individual, uncoupled rate. Practical limits on spatial resolution also imply that the convective heat transfer to the walls of the vessel must be treated by wall function or boundary-layer correlation methods. For control-volume models, the relatively small number of volumes used in most simulations requires that the *average* gas state be used in these correlations instead of the *local values*. It is in the spirit of these simple models that we would like to examine each individual process and determine what scaling relations apply.

For the present study, we consider only the issues associated with computing the average heat transfer rates due to thermal radiation and convection alone. As pointed out below, the problem of determining the local heat transfer rate to a small item at a particular location in the containment is a much more difficult and, possibly, even more important problem. In addition, condensation-evaporation phenomena will be ignored, although for high steam concentrations and cases in which water sprays are present, they can be extremely important heat transfer mechanisms.

Under the assumptions and limitations outlined above, the average gas temperature T_g can be calculated for post-combustion times from a global energy balance

$$V\rho C_v \frac{dT_g}{dt} = -A\sum q_i, \quad \text{and} \quad T_g(t=0) = T_m, \qquad (1)$$

where q_i are the different heat transfer mechanisms of importance, *i.e.*, convective, radiative, and condensation fluxes. The burn is considered to occur instantaneously and the postcombustion heat transfer starts at time $t = 0$. T_m is the temperature at the end of burn, which is $\sim 85\%$ of the adiabatic isochoric combustion (AIC) value for the tests discussed in this report. The 15% decrease indicates the fraction of energy transferred during the burn. For the sake of simplicity, thermophysical properties are assumed to be constant in the scaling relations, with a few exceptions (notably the volumetric coefficient of expansion). All characteristic length scales that enter into the scaling relations will be referred to by the same symbol, S, which can be thought of as the equivalent diameter of the vessel. By inspection, Eq.(1) can be used to define a characteristic time scale (τ) for the gas cool-down process. This time scale is the ratio of the maximum energy loss rate to the initial energy in the gas

$$\tau_i = \frac{V\rho C_v T_m}{A q_i}. \qquad (2)$$

A small time scale implies a greater rate of energy removal by that mechanism. Comparison of the relative magnitudes of τ_i thus determines the importance of the various mechanisms.

Thermal Radiation

Given our remarks above, an appropriate model for thermal radiation from the combustion products (steam) would be that the gas temperature is uniform, the enclosure is black and cold, and re-radiation is negligible. The radiative heat flux is

$$q_r = -\epsilon_g(\mathcal{L}, P, T_g, \overline{x})\sigma T_g^4. \qquad (3)$$

As stated, the only significant unknown in Eq.(3) is the gas emittance, ϵ_g, which is a function of the gas temperature, pressure P, and composition $\overline{x}$, and the characteristic radiation length $\mathcal{L}$ (referred to as the beamlength).

We have calculated the emittance with the exponential wide-band model of Edwards[6] and other emittance relations[7] (including the Hottel charts and the Cess-Lian correlation) for steam using gas pressures, temperatures and compositions (oxygen-nitrogen-water mixtures) appropriate to AIC conditions for initial hydrogen concentrations ranging from 10–30% in dry air. Quite conveniently, the emittance appears to be nearly independent of the initial hydrogen concentration, as shown in Figure 1. Similarly, we have calculated the variation of emittance during a constant volume cool-down process and find that it is also essentially constant. These fortuitous results enable us to use a simple correlation that depends only on the beamlength $\mathcal{L}$:

$$\epsilon_g \simeq 0.087 \ln(31.5\mathcal{L}); \quad (0.1m \le \mathcal{L} \le 10.m). \qquad (4)$$

For enclosures, the appropriate beam length can be determined once the geometry of the vessel is fixed. An often-used approximation[7] is

$$\mathcal{L} = 3.5\frac{V}{A} \propto S. \qquad (5)$$

With these simplifications, the energy equation (Eq.(1)) for radiative transfer only can be solved exactly,

$$\frac{T_g}{T_m} = \left(1 + 3\frac{t}{\tau_r}\right)^{-1/3}, \qquad (6)$$

where τ_r is the characteristic thermal radiation time scale. This equation is only valid for $T_g \gg T_w$, *i.e.*, at early times. Note that for a fixed initial hydrogen concentration (or T_m), the time scale τ_r depends only on the mean beam length and scales as $\tau_r \propto S/\ln S$.

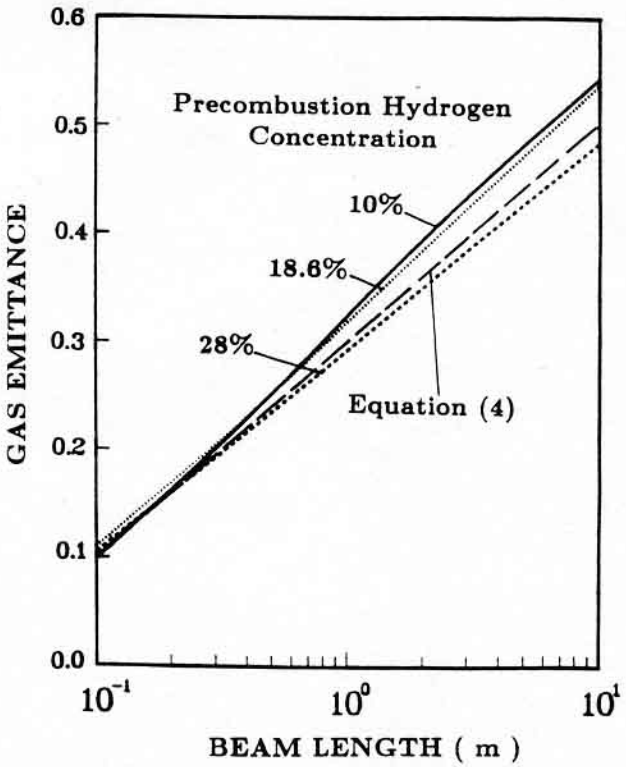

Figure 1. Gas emittance dependence on the beam length

Convection

Due to the transient nature of deflagrations and the natural decay of the induced fluid velocity, different modes of convective heat transfer are important at different times. Initially, the velocities and turbulent intensities caused by the buoyant rise of the growing fireball and the flame-flowfield interactions are quite large compared to typical natural convection velocities. This can result[8] in peak heat transfer coefficients as high as 40 - 50 W/m^2-K. Immediately after the burn, the velocity begins to decay due to dissipation within the fluid and at the walls. Eventually, the heat transfer process will become dominated by either forced convection (if fans are operating) or natural convection.

In general, the convective heat flux q_c is determined from an engineering correlation for the heat transfer coefficient h,

$$q_c = h\,(T_g - T_w)\,. \tag{7}$$

Typically, values of h are calculated for each of the different modes of convection and the highest value is used. While this may appear to be arbitrary, it serves to define the crossover time between transient and forced or natural convection. Each of the possible convective modes are discussed below. Representative correlations included in HYBER[5] are used in these discussions.

Transient Convection

The basic difficulty with computing the transient convection is that the characteristic fluid velocity at the end of the burn is unknown and also nonuniform. In addition, the decay process and transition to natural or forced convection is not well enough understood to make calculations for arbitrary vessels. However, there does exist a simple correlation[9] developed for heat transfer following the transient injection of hot gas into small-scale vessels ($\sim$ 0.1 m^3). This correlation relates the Nusselt number Nu, to the Fourier number Fo,

$$Nu = 0.28Fo^{-0.74};\quad Nu = \frac{hL}{k};\quad Fo = \frac{\alpha t}{L^2}. \tag{8}$$

L is the characteristic flow length scale, chosen to be the diameter of the vessel.[9] Using this relation for h in the energy equation, the solution is

$$\Delta T = \Delta T_m \exp\left(-C\left(\frac{t}{\tau}\right)^{0.26}\right);\quad \tau = \frac{L^2}{\alpha} \tag{9}$$

where C is a constant of $\mathcal{O}(1)$, $\Delta T = T_g - T_w$, and $\Delta T_m = T_m - T_w$.

It is impossible to define a meaningful time scale for this process, due to the time dependence. What is important instead is the duration of the transient period (Δt_{tc}). Unfortunately, Δt_{tc} depends on the gas temperature–time history and must be determined for each length scale. The only general statement that can be made is that Δt_{tc} increases rapidly with scale.

While this correlation has been used to model experimental results,[5] there are several difficulties inherent in this formulation. Clearly, the correlation cannot be valid at time $t = 0$. Although the singularity can be avoided by starting the computation at a small but finite time, this still leaves the peak value of the flux undetermined. This difficulty is directly related to our inability to define a characteristic velocity at the end of the burn. The resolution of the problem will require a more detailed analysis of the combustion process and possibly, further experimentation.

Natural Convection

Natural convection is usually handled by a boundary layer or enclosure correlation. For turbulent free convection, one correlation is

$$Nu = 0.12Ra^{1/3};\quad Ra = \frac{g\beta\rho\Delta T L^3}{\alpha\nu}, \tag{10}$$

where L is the characteristic *vertical* scaling length for buoyancy.

If it is assumed that all gas thermophysical properties are constant except for the coefficient of volumetric expansion β (assumed $= 1./T_g$), then a closed-form solution to the energy equation can be obtained. However, since gas property variations are substantial during cool-down, such an analysis is not warranted. Instead, approximate relations obtained for the two limiting cases of $T_g \gg T_w$ (*i.e.*, $\Delta T/T_g \sim \mathcal{O}(1)$) and $T_g \approx T_w$ (*i.e.*, $\Delta T/T_g \ll 1$) are more useful for characterizing the phenomena.

For $\Delta T/T_g \sim \mathcal{O}(1)$, at early times, the Rayleigh number is essentially constant and the solution to the energy equation is

$$\Delta T = \Delta T_m \exp\left(-\frac{t}{\tau_{nc}}\right). \tag{11}$$

For $\Delta T/T_g \ll 1$, at late times, $Ra \propto \Delta T$ and the solution to the energy equation is

$$\Delta T = \Delta T_m \left(1 + \frac{t}{\tau_{nc}}\right)^{-3} \tag{12}$$

For both limits, the characteristic natural convection flux is defined as

$$q_{nc} = 0.12\frac{\alpha\Delta T_m}{\ell_{nc}} \tag{13}$$

where ℓ_{nc} is the intrinsic natural convection scaling length defined by setting the Rayleigh number based on T_m equal to unity and solving for the length scale $L = \ell_{nc}$.

Note that the difference in the two limits is due to the behavior of the expansion coefficient $\beta = 1/T_g$. For either limit, the time constant scales as $\tau_{nc} \propto S\Delta T_m^{1/3}$. In addition, both the characteristic heat flux and length scale are independent of the size of the vessel. For the 10% (nominal) hydrogen burns considered in this work, $\ell_{nc} = 0.7$ mm and $q_{nc} = 1.2$ W/cm^2.

Forced Convection

Forced convection is typically treated with a flat-plate, turbulent boundary layer correlation based on the Reynolds number. The relation used in HYBER is

$$Nu = 0.37 Pr^{0.6} Re^{0.8}; \quad Pr = \frac{\nu}{\alpha}; \quad Re = \frac{UL}{\nu}. \qquad (14)$$

In order to use this correlation, the characteristic mean velocity U, and the effective boundary layer length L, must be known. In reality, this correlation is rarely appropriate for the flows and geometries of either experiments or containment simulations. An enclosure formulation, based on the mean circulation rate, would be much more realistic; unfortunately, there are no data (experimental or numerical) at the scales of interest. Many times these correlations are used with length scales and velocities chosen to match experimental results instead of using the transient convection correlation discussed above. If there was a basis for choosing a scaled flowrate and length, this type of model could also be used for simulating the effect of containment fan coolers.

For a given velocity and length scale, the solution to the energy equation is

$$\Delta T = \Delta T_m \exp\left(-\frac{t}{\tau_{fc}}\right). \qquad (15)$$

The characteristic time constant scales as $\tau_{fc} \propto U^{-0.8} \mathcal{S}^{1.2}$, since the heat transfer coefficient $h \sim U^{0.8} L^{-0.2}$.

3 Issues

As indicated in the previous section, modeling of the coupled heat transfer and fluid dynamic phenomena during and following combustion is difficult, and typically is not attempted. Instead, the processes are decoupled, and the individual contributions are treated as noninteracting, but competing effects. These contributions are then summed to obtain the total heat transfer. Standard engineering correlations for steady-state convective heat and mass transfer are then also used, neglecting early-time decaying gas flow and turbulence induced by the combustion. In addition, most nuclear-safety codes model large open areas as single control volumes, so that *global* instead of *local* phenomena are predicted. This formulation is sufficient for prediction of gas pressure histories necessary for assessing containment integrity, but may be inadequate for resolving the issue of safety-related equipment survival.

Given the modeling shortcomings discussed above, there is always a large margin of uncertainty applied when using global simulations in reactor-safety analyses. Fortunately, as shown in the Results section, global formulations are sufficient in many cases for scoping problems, as long as the modeler remains cognizant of the limitations of these simulations. It is important that such global models be validated using experimental results for simple configurations, and that global versus local issues be resolved using experimentation, whenever possible.

Resolution of local versus global issues by experimentation is complicated by the difficulty in measuring local phenomena, as is shown in Figure 2.[10] Measured peak heat fluxes are shown for several different types of calorimetry included in 21 premixed combustion experiments performed in the NTS hydrogen dewar. Local instrumentation available in these tests included off-the-shelf Gardon and Schmidt-Boelter gauges, as well as SNLA-fabricated resistance thin-film gauges, slug and cube capacitance calorimeters. These instruments were all positioned in the upper half of the spherical dewar, and the heat transfer measurements from all gauges were expected to be comparable. The lower hydrogen concentration (less severe) tests were performed first, and the hydrogen concentration was increased as testing proceeded.

As can be seen from the figure, the differences in measured heat transfer results increased with increasing test severity, indicated by the shaded region. From this figure, it should be apparent that quantifying local effects is difficult in large-scale facilities, and that global representations of the phenomena may have to suffice. It is also questionable whether the local data are accurate and sufficiently complete to be used to validate more sophisticated finite-difference or finite-element field equation computer simulations.

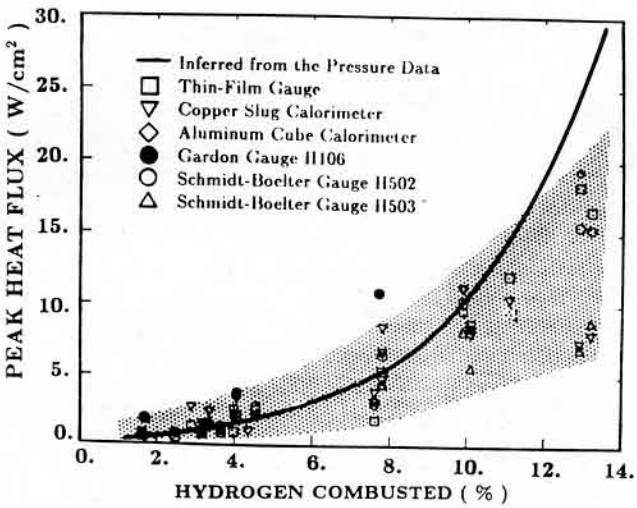

Figure 2. Comparative peak heat fluxes from NTS premixed combustion experiments

4 Combustion Experiments

Test Facilities

The combustion tests analyzed in this work were conducted in the 5.6 m^3 Fully Instrumented Test System (FITS) facility at SNLA[11,12] and in the 2084 m^3 hydrogen dewar at NTS.[3,10] The former facility is a cylindrical steel vessel and the latter is a stainless steel sphere. Testing at NTS was funded jointly by the NRC and the Electric Power Research Institute (EPRI) and tests were performed by personnel from EPRI and subcontractors. Additional instrumen-

tation for quantifying the environment in the NTS dewar were provided by SNLA. All FITS testing was performed by SNLA personnel and contractors. Table 1 provides additional specifications for the two test facilities. Note that characteristic lengths used for modeling radiative and convective heat transfer in these vessels are also given in this table.

Table 1. Combustion Test Vessel Data

Specification	Test Facility	
	FITS	NTS
Geometry	Cylinder	Sphere
Enclosed Volume	5.6 m^3	2084. m^3
Surface Area	19.5 m^2	789. m^2
Diameter	1.45 m	15.8 m
Wall Thickness	25. mm	25. mm
Characteristic Lengths		
Radiation	1.2 m	10.6 m
Conventional Convection*	3.4 m	15.8 m
Transient Convection†	1.45 m	15.8 m

* Used in forced convection correlation
† Used in transient convection correlation

Instrumentation and Data Processing

Instrumentation used in the two test facilities included pressure sensors, gas and wall thermocouples, and calorimetry for measuring total and radiative heat transfer. Gas velocity probes were also provided for the NTS combustion experiments; unfortunately, these instrumentation were inoperable or provided suspect data for most of the testing program. Results from pressure sensors and total thin-film gauges are included in this work; descriptions and data reduction procedures used in the SMOKE data reduction computer models for these instrumentation[13] are outlined below.

Pressure Sensors

Pressure sensors used at FITS and at NTS were of the strain-gauge type. The gauges were installed inside FITS, and the sensing elements were actively air-cooled and also thermally shielded with felt-metal insulation. The gauges used at NTS from which our data were obtained were located outside of the dewar at the end of a tube which extended into containment and provided communication with the gas.

Pressure data not only provide the gas pressure response during the experiment, but can also be used to infer information about the average heat transfer following combustion. In this technique, as first applied by Means and Ulrich,[9] the total rate of heat loss from the gas is proportional to the time derivative of the pressure and the radiative loss rate is related to the absolute pressure. The convective losses are equal to the difference between the total and radiative components with a correction for condensation if necessary as given in Eq.(16):

$$q_c = q_t - (q_r + q_{cond}). \tag{16}$$

For tests in which wall condensation effects are expected to be minimal, the total heat transfer rate is related to the pressure derivative according to Eq.(17),

$$q_t = -\frac{C_v}{R}\frac{V}{A}\frac{dP}{dt}. \tag{17}$$

It is assumed that the combustion is completed at the time of peak pressure, and that the gas composition is constant and identical to that computed for an AIC process. This is assumed since the gas composition is not measured after completion of combustion (and, for tests where condensation effects are important, is not measured at various times during the postcombustion cooling process).

The average radiative heat transfer rate can also be estimated from the gas pressure since the average gas temperature can be calculated from the ideal gas equation of state. The radiative heat transfer is then calculated as

$$q_r = \sigma(\epsilon_g T_g^4 - \alpha_g T_w^4). \tag{18}$$

The walls are assumed to be black, and are allowed to heat-up by absorption of the total heat loss from the gas during and following combustion. Both the gas absorptance ($\alpha_g = \alpha_g(\mathcal{L}, P, T_g, T_w, \bar{x})$) and emittance ($\epsilon_g = \epsilon_g(\mathcal{L}, P, T_g, \bar{x})$) are computed with the exponential wide-band model.[7] Note that this data analysis procedure is different from the simple scaling relations, where the gas properties were assumed constant and the wall temperature was assumed to be constant and 'cold' relative to the gas.

The analysis is complicated when condensation occurs on the vessel walls, since the time rate of change of the steam mass must be accounted for in the the state equation and in the total heat transfer rate. The steam concentration in this case has to be inferred from the pressure data because it is not measured. This is done using the extended Chilton-Colburn analogy[14] to relate mass transfer and convective heat transfer. For these analyses, the state, conservation, and rate equations are coupled and must be solved simultaneously. The radiative heat transfer calculation is also complicated by the dependence of the gas temperature and radiative properties on the gas composition. A more detailed description of this analysis is given in Reference 13.

Total Thin-film Gauge

Total thin-film gauges, developed at SNLA, were used in the two test programs for transient heat flux measurements. They consisted of a 300 Angstrom-thick platinum resistance element 2.5 mm wide and 13 mm long mounted on a synthetic glass ceramic substrate (MACOR) 0.10 m in diameter. The exposed surface of the gauge was coated with a spectrally-flat, highly-absorptive black paint, and the back surface was insulated. The calorimeter bodies were also installed in a protective stainless-steel housing. The total

thin-film gauges were positioned on the cylindrical wall near the top of FITS and at the top of the dewar at NTS.

These gauges are modeled as one-dimensional devices, with temperature variations perpendicular to the gauge front surfaces. Using the thermal properties of the MACOR and the measured front-surface temperatures, the front-surface heat flux is computed by numerically solving the transient conduction problem for a one-dimensional, semi-infinite slab[13] Note that the gauge front surface is sufficiently cool relative to the combustion gases so that re-radiation losses are negligible for the times of interest.

Experimental Procedures

The combustion experiments were performed at FITS and NTS in the following manner: The test vessels were preheated to some desired condition using steam. Fans were used in FITS during preheating and both water sprays and fans were used at NTS. Following preheating, prescribed quantities of hydrogen and steam, as determined by the static pressure increase, were introduced and allowed to equilibrate with the air already present in the vessel. Fans and sprays were used to bring the gas to equilibium. Once the gas was sufficiently mixed and the gas and wall temperatures were equilibrated, a spark or glow plug(s) were energized, initiating combustion. Additional information about the experimental procedures and instrumentation are given in References 11 and 12 for the FITS tests and in References 3 and 10 for the NTS tests.

5 Results

In this section, comparisons of results from two 10% (nominal) hydrogen combustion tests performed at FITS (test H10H) and at NTS (test NTSP15) are provided, along with results from the simple scaling relations and from HYBER simulations. Fans and sprays were turned off prior to combustion for both tests. Wall temperatures were initially low ($\sim$ 300 K) in test NTSP15 so that condensation effects needed to be accounted for in the pressure data analyses and in modeling. Test H10H had an elevated wall temperature ($\sim$ 350 K) and condensation effects were minimal. Additional precombustion conditions for these tests are summarized in Table 2. Note that these tests were selected as representative from our work with FITS and NTS data,[5,10] as are the conclusions which will be presented.

The HYBER computer simulation used in this work was developed in support of NRC evaluations of safety-related equipment performance when subjected to degraded core accidents in nuclear reactor containments.[5] It has also been used to model combustion experiments performed at SNLA. HYBER utilizes a transient lumped volume model to simulate combustion and postcombustion thermal environments in single physical compartments, providing gas state histories and vessel and included equipment thermal responses. Heat and mass transfer correlations are used, as is a radiation model which includes surface exchange and gas radiative transfer. Gas emittances needed in the radiation model are computed from the Cess-Lian emittance model[7] using the current gas state for each time step. Gas thermophysical properties needed in the heat and mass transfer correlations and in the gas energy conservation relation are computed for the different species comprising the gas from kinetic theory models and tabulated data. Mixture theory models based on mole fraction weighting are used to compute gas mixture properties. For additional information on HYBER, the reader should refer to the HYBER reference manual.[5]

Table 2. Precombustion Conditions for Tests

Condition	Test Designation	
	H10H	NTSP15
Gas Pressure	94.1 kPa	109.3 kPa
Gas Temperature	352.1 K	303.4 K
Hydrogen Concentration	10.2%	9.9%
Steam Concentration	4.0%	4.2%
Combustion Completeness	100%	100%
Ignition Source	Glow plug	Glow plug
Ignition Location	Bottom	Bottom
Combustion Duration	1.24 s	3.60 s

Comparative Experimental Results

Pressure histories for the two tests are compared in Figure 3. The pressure decay is much faster for test H10H than for NTSP15. This is also reflected in the total heat transfer rates obtained from the thin-film gauges (Figure 4) and in total and radiative heat transfer rates inferred from the pressure (Figure 5). The total heat transfer rates remain high in test NTSP15 for significantly longer times than in H10H. This should be anticipated from our scaling analysis, since the characteristic time scales all increase with increasing scale. Comparisons of the peak conditions from these tests are summarized in Table 3.

Table 3. Peak Pressures and Heat Fluxes

Peak Condition	Test Designation	
	H10H	NTSP15
Gas Pressure and Temperature		
Measured Pressure Ratio (P_m/P_0)	2.95	3.61
AIC Pressure Ratio (P_m/P_0)	3.51	4.14
Measured Temperature Ratio (T_m/T_0)	3.33	3.81
AIC Temperature Ratio (T_m/T_0)	3.98	4.35
Heat Flux Results (W/cm^2)		
Total: Thin-film Gauge	8.99	10.29
Total: Inferred from Pressure	6.49	10.58
Radiative: Inferred from Pressure	3.29	5.94
Condensation: Inferred from Pressure	~0.0	1.30
Convective: Inferred from Pressure†	3.20	3.34

† Convective heat flux obtained from Eq.(16)

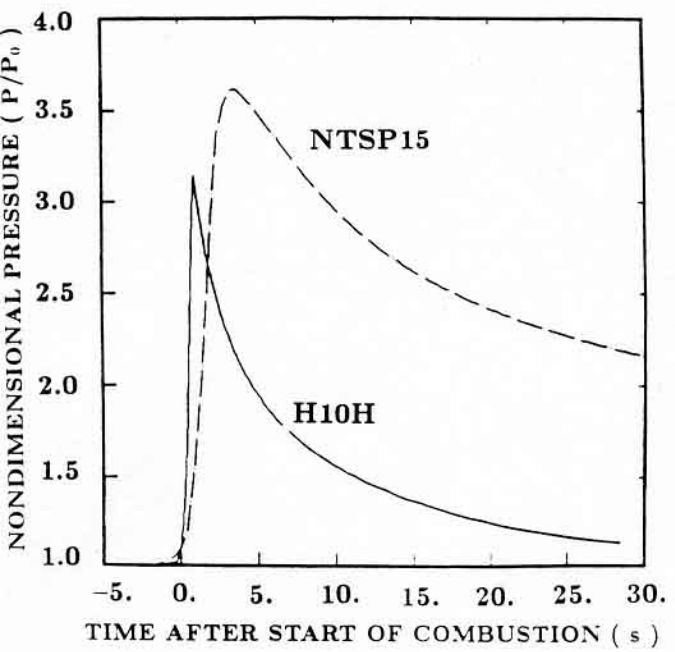

Figure 3. Comparative pressure results for tests H10H and NTSP15

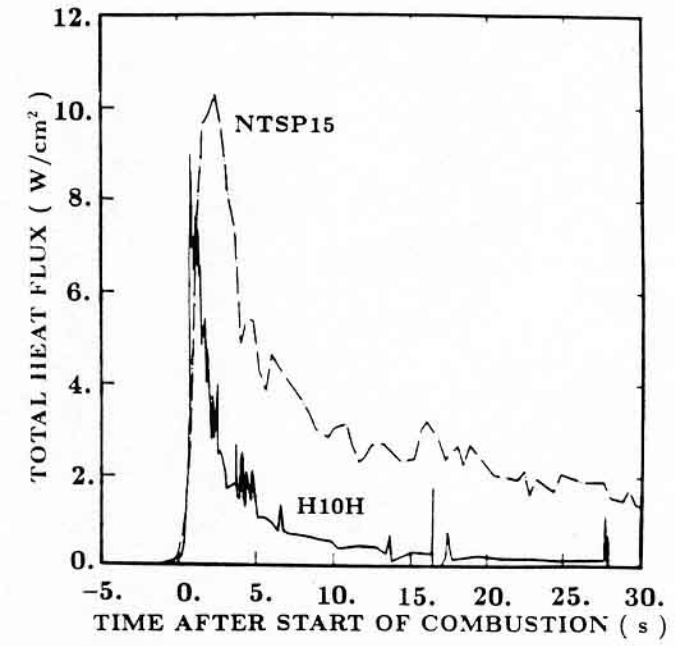

Figure 4. Comparative total heat fluxes measured by the thin-film gauges

The differences in peak total heat fluxes for the two tests are only slightly less than the differences in the peak radiative fluxes. Enhanced radiative transfer would be expected from the scaling relations for gas emittance, since the increase in the characteristic radiative length scale from 1.2 m in FITS to 10.6 m in the NTS dewar results in a factor of 2 increase in the gas emittance from ~ 0.3 to ~ 0.6. The additional increase in the total flux suggests that the convective heat transfer may be slightly enhanced (*e.g.*, more turbulence) in test NTSP15. Although this effect might be anticipated due to the more pronounced effect of buoyancy in the larger vessel, it is not as large as we might expect due to uncertainties in the local measurements. For example, the peak heat flux from the total thin-film gauge for test NTSP15 is probably low. The data acquisition system used at NTS did not record data sufficiently often for accurate resolution of the peak flux; we believe that the maximum flux was probably 1-3 W/cm^2 greater than recorded.[10]

Comparisons of the local thin-film results and the global results from the pressure in Figures 4 and 5 and in Table 3 are quite good for each test alone. Local peak heat fluxes are comparable to the average values, which might be expected (given the locations of the thin-film gauges in the vessels), and the decays are also quite similar. These trends have been reported previously for tests performed in the intermediate FITS vessel,[14] and are also demonstrated in Figure 2 for the NTS premixed combustion tests. In the latter case, the heat transfer and energy deposition are consistent with the measurements for the less severe tests and are greater than the measurements for the more severe tests when instrumentation performance was suspect.[10]. This indicates that, at least for the two geometries considered here, the average total heat transfer can be used in the absence of local calorimetry results for quantifying the heat load on the vessel. Note that for lean hydrogen deflagrations (< 6–7%), the good agreement may have been fortuitous (*i.e.*, because of the locations of instrumentation in upper part of the dewar), since local effects would be expected to be more important for incomplete combustion tests.[10]

In general, global quantities computed from the pressure have been found to compare well with local measurements of gas temperatures, wall temperatures, and heat fluxes recorded for FITS and NTS combustion tests. As an example, Figure 6 provides a comparison of measured gas temperatures and global gas temperature predictions for test NTSP15. The 3-mil and 32-mil thermocouples were located near the top and near the center of the NTS dewar, respectively. Such good agreement was typical for all NTS tests where the combustion was nearly complete,[10] and also for the combustion tests performed in the FITS vessel.

Scaling Results

The various scaling relations and numerical values of time scales and characteristic fluxes are given in Table 4 for the combustion tests in the two test vessels. Several conclusions are obvious from these results. Thermal radiation rapidly becomes the dominant mechanism as the initial temperature T_m (related to initial hydrogen concentration) increases. This is due to the strong dependence of the thermal radiation time scale on T_m and the very weak dependence (or independence) of the convective time scales on T_g. At very long times after combustion, convective mechanisms must eventually dominate; but the duration of the

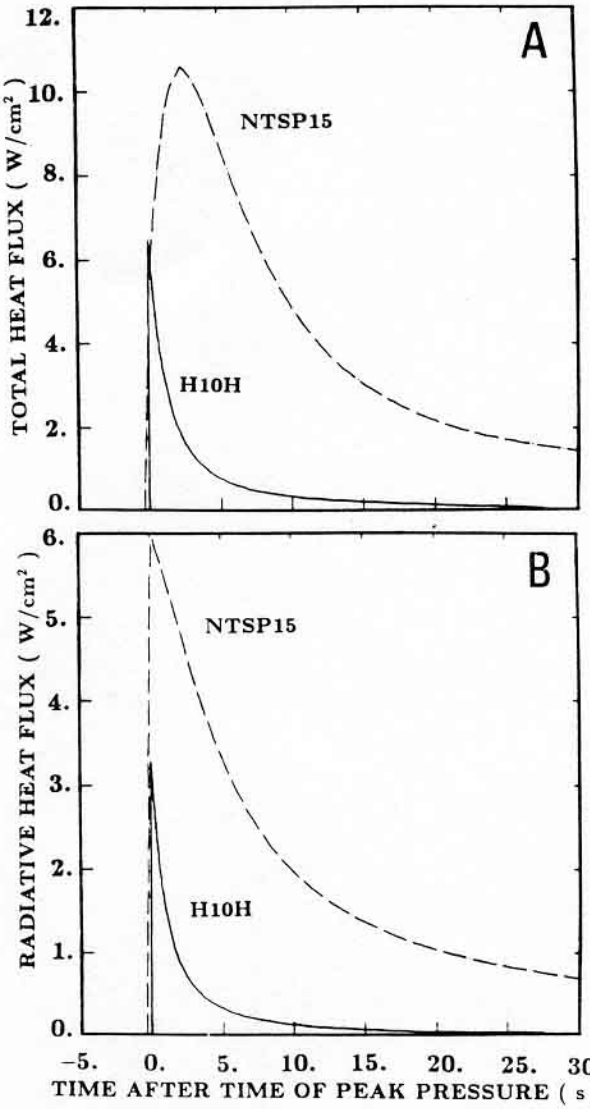

Figure 5. Comparative total (A) and radiative (B) heat fluxes inferred from the pressure data

radiation-dominated stage also increases as T_m increases.

The importance of thermal radiation increases only weakly (as $\ln S$) compared to natural convection as a function of scale for fixed hydrogen concentration. Therefore, we would expect that the relative contributions of these two mechanisms would be only weakly dependent on scale. As a rough guide, the characteristic time for the gas cool-down due to the combined mechanisms should increase approximately proportionally to S for a fixed initial hydrogen concentration. These relations are approximately satisfied for both the NTS and FITS combustion experiments considered in this work.

Finally, it is obvious that the boundary-layer forced convection models do not give a realistic time scale when typical velocities (< 10 m/s) are used. This indicates that this type of mechanism will almost never be important at early times following combustion and that heat transfer at long times will be dominated by natural convection. However, fans

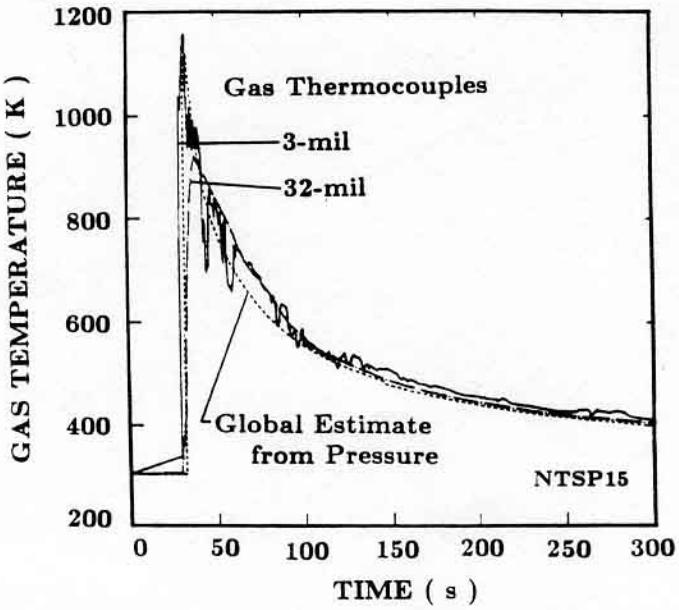

Figure 6. Gas temperatures for test NTSP15, measured and inferred from the pressure

Table 4. Characteristic Times and Fluxes for Scaling Relations

Heat Transfer Mechanism	Time-Scale Dependence	Experimental Test Facilities			
		NTS Dewar		FITS Cylinder	
		τ_i (s)	q_i (W/cm²)	τ_i (s)	q_i (W/cm²)
Thermal Radiation	$S\,(T_m^3 \ln S)^{-1}$	11.6	3.2	66.3	5.1
Natural Convection	$S\Delta T_m^{-1/3}$	30.9	1.2	281.6	1.2
Forced Convection*	$S^{6/5}U^{-4/5}$	100	0.37	1254	0.27
Transient Convection†	S^n $(1/2 \le n \le 2)$	$\Delta t_{tc} \simeq 5$ s		$\Delta t_{tc} \simeq 20$ s	

Values are based on a gas temperature of 1155 K and a composition of $x_{H_2O} = 0.15$, $x_{O_2} = 0.13$, and $x_{N_2} = 0.72$. Associated thermophysical properties are as follows: $\rho = 1.109$ kg/m³, $C_v = 1000$ J/kg-K, and $\nu = 4.114 \times 10^{-5}$ m²/s

* Results provided for steady free-stream gas velocity of 10 m/s

† Estimated duration of transient convection provided

NB These two columns switch

can have a strong local effect *during* the burn and cause an acceleration of the flame through enhanced turbulence.

Experimental Data and HYBER Results

Comparisons of experimental results and three HYBER simulations of the pressure decay using the different heat transfer mechanisms for tests H10H and NTSP15 are given in Figures 7 and 8, respectively. In addition, comparisons of

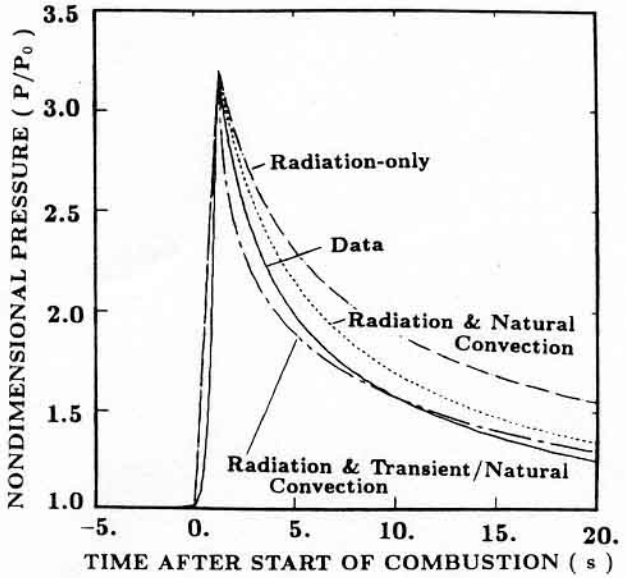

Figure 7. Pressure data and HYBER simulations of test H10H

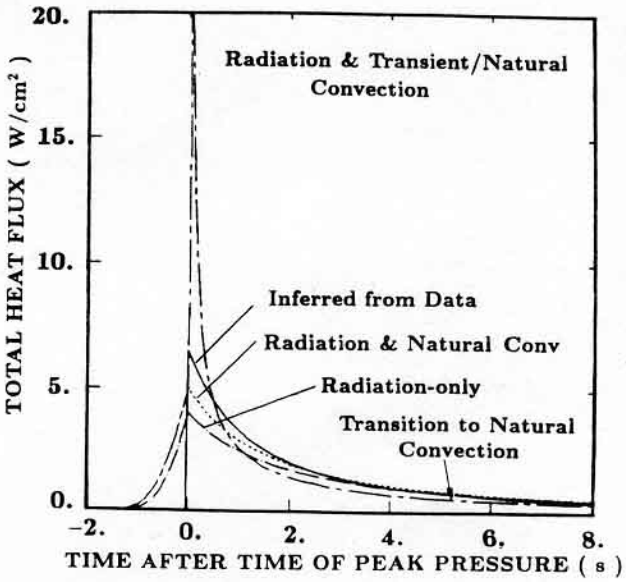

Figure 9. Total heat flux comparisons for test H10H

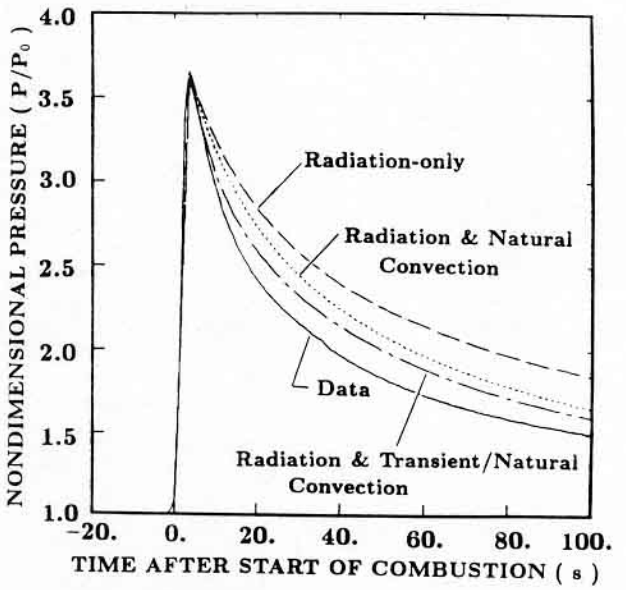

Figure 8. Pressure data and HYBER simulations of test NTSP15

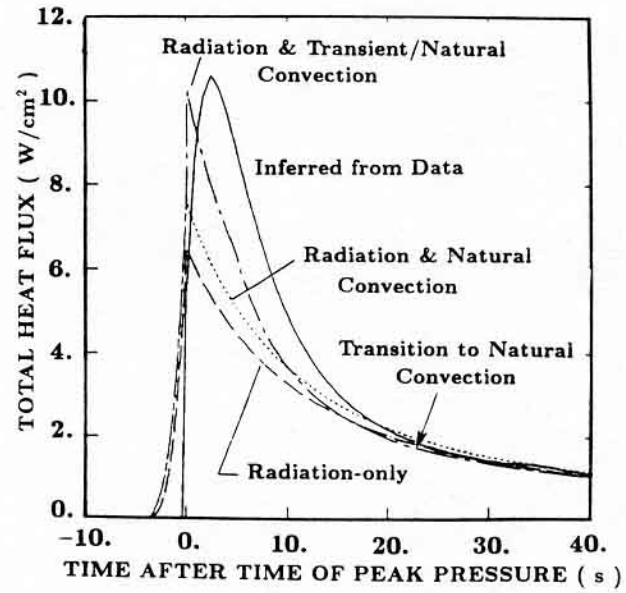

Figure 10. Total heat flux comparisons for test NTSP15

the total heat flux profiles from HYBER and inferred from the pressure are given in Figures 9 and 10 for the two tests. Included in the HYBER simulations are: (1) radiation-only energy transfer; (2) radiation and natural convection energy transfer; and (3) radiation and transient/natural convection energy transfer. In the latter calculation, HYBER computes both the transient and natural convection flux and uses the larger value. The arrows shown in Figures 9 and 10 indicate the transition from transient to natural convection, as computed in HYBER. The forced convection correlation comparison is omitted, since fans were not operating in these tests.

The combined mode HYBER simulations bracket the experimental pressure results for H10H and all estimates underpredict the heat transfer for NTSP15. In H10H, the transient convection correlation over-predicts the early-time convection, while the natural convection correlation underpredicts convection for both tests. The radiative components (not shown) predicted from the combined mode HYBER simulations are comparable with the global radiative heat fluxes at all times. The late-time pressure for the two combined mode simulations and the data are also comparable, indicating that the natural convection cooling model is appropriate. At these times, the gas is sufficiently cool

that the radiative transfer is negligible. Note that either the radiation or natural convection alone are insufficient for predicting the data for either test.

Despite the apparent success of the Means and Ulrich correlation, the functional form does not appear appropriate for a turbulent heat transfer mechanism. The appearance of the thermal diffusivity (Fourier number) in the correlation may be misleading since this relation has only been tested at essentially one (very small) length scale. Further data reduction and analysis of more experiments is needed to fully understand the limitations of this model.

6 Summary

We have considered the issues associated with modeling postcombustion radiative and convective heat transfer. The importance of scale has been shown through a simple scaling analysis for the individual heat transfer mechanisms. Results from two 10% hydrogen deflagration experiments performed in the 5.6 m^3 FITS and 2084 m^3 NTS dewar test facilities were used to demonstrate scaling concepts and to emphasize the importance of scale.

Average total and radiative heat fluxes were inferred from the measured pressure data. Good agreement was found between the average total fluxes and measurements obtained with thin-film calorimeters. With some reservations, the pressure-inferred fluxes have been shown to be useful for assessing nuclear reactor-safety simulation models. There is still concern, however, that for cases where local phenomena are important, as in resolving equipment survival issues, better local experimental data are needed.

We also compared the postcombustion pressure decays for the two tests with the results of HYBER simulations. Although the scaling relations provided valuable insight to the gas cooling phenomena, the importance of the combined effects of the heat transfer mechanisms was evident. Computed pressures using the combined transient convection and radiation models were comparable to the data for both tests. Deficiencies in modeling convection heat transfer were shown to occur at early times following combustion. The conventional Reynolds number correlation for forced convection was shown to be inappropriate from the simple scaling analysis. Instead, a transient convection model similar to the Means-Ulrich correlation is needed. The average late-time convection heat transfer appears to be adequately modeled using a conventional turbulent natural convection correlation.

Acknowledgements

This work was performed in support of the Hydrogen Burn Survival and Hydrogen Behavior Programs at Sandia National Laboratories, Albuquerque, New Mexico. J. Haugh of EPRI and S. F. Roller of SNLA were responsible for the testing described in this paper. S. N. Kempka was involved in the development of HYBER and SMOKE.

References

1. Henrie, J. O., and Postma, A. K. ,*Analysis of the Three Mile Island (TMI-2) Hydrogen Burn*, Report RHO-RE-SA-8, Rockwell International, GEND-INF-023, Vol. IV, March, 1983.

2. Baer, M. R., Griffiths, S. K., and Shepherd, J. E., *Hydrogen Combustion in Aqueous Foams*, Nuclear Science and Engineering, Vol. 88, 1984, pp. 436-444.

3. Thompson, R. T.,*et al., Large-Scale Hydrogen Combustion Experiments*, Electric Power Research Institute Report NP-3878, in preparation.

4. Camp, A. L., Wester, M. J., and Dingman, S. E.,*HECTR Version 1.0 Users' Manual*, Sandia National Laboratories Report SAND 84-1522, February, 1985.

5. Kempka S. N., and Ratzel, A. C.,*Reference Manual for HYBER, the Hydrogen Burn - Equipment Response Algorithm*, Sandia National Laboratories Report SAND 84-0160, June, 1984.

6. Edwards, D. K.,*Molecular Gas Band Radiation*, Advances in Heat Transfer, Vol. 12, Academic Press, New York, 1976.

7. Siegel, R., and Howell, J. R.,Thermal Radiation Heat Transfer, 2nd Ed., McGraw-Hill Book Company, New York, 1981.

8. Kempka, S. N., *et al., Postcombustion Convection in an Intermediate-Scale Vessel*, Proceedings of the Joint ASME/ANS Conference on the Design, Construction, and Operation of Nuclear Power Plants, Portland OR, August 5-8, 1984.

9. Means, J. D., and Ulrich, R. D., *Transient Convective Heat Transfer During and After Gas Injection into Containers*, Trans. ASME J. Heat Transfer, 97, No.2, 1975, pp. 282-287.

10. Ratzel, A. C., *Data Analysis for NTS Premixed Combustion Tests*, Sandia National Laboratories Report SAND85-0135, April, 1985.

11. Roller, S. F., and Fallacy, S. M., *Medium-Scale Tests of H_2:Air:Steam Systems*, Proceedings of the Second International Conference on the Impact of Hydrogen on Water Reactor Safety, Albuquerque, N. M., October 3-7, 1982.

12. Marshall, B. W., and Ratzel, A. C., *Pressure Measurements in a Hydrogen Combustion Environment: An Evaluation of Three Pressure Transducers*, Sandia National Laboratories Report SAND83-2621/2 of 2, May, 1984.

13. Ratzel, A. C., *et al., SMOKE: A Data Reduction Package for Analysis of Combustion Experiments*, Sandia National Laboratories Report SAND83-2658, May, 1985.

14. Bird, R. B., Stewart, W. E., and Lightfoot, E. N., Transport Phenomena, John Wiley and Sons, Inc., New York, 1960.